UNIVERSITÉ CATHOLIQUE DE LOUVAIN

Study of the stress relieve heat-treatment of additively manufactured AlSi10Mg alloy:

Influence on microstructure and mechanical properties

Dissertation presented by

David DISPAS   *and*   Arthur BOUILLOT

for obtaining the Master's degree in

Mechanical Engineering   *and*   Chemical and Materials Engineering

at Ecole Polytchnique de Louvain (EPL)

Supervisor: Aude SIMAR

Readers: Laurent DELANNAY, Anne MERTENS, Camille VAN DER REST

Academic year 2017-2018

'Citation stylée.'

Mec cool

Acknowledgements

Gros betch à mes poules Aude Simar et Camille Van Der Rest et aux potos du labo

Contents

List of Figures

List of Tables

List of Abbreviations

AM   Additive Manufacturing
CAD   Computer Aided Design
DMLS   Direct Metal Laser Sintering
DMP   Direct Metal Printer
ICP   Inductively Coupled Plasma
SEM   Scanning Electron Microscope
SLM   Selective Laser Melting

Symbols

D_a	Average particle size	$[\mu m]$
E_d	Volumetric energy density	$[\frac{J}{mm^3}]$
h	Hatch space	$[\mu m]$
P	Laser power	$[W]$
p_{O_2}	Oxygen pressure	$[mbar]$
t	Layer thickness	$[\mu m]$
v_s	Scanning speed	$[\frac{mm}{s}]$
$\phi_{99\%}$	Laser spot size at the 99% contour	$[\mu m]$
λ	Laser wavelength	$[nm]$
ρ_{rel}	Apparent relative density	$[-]$

Nous dédions ce travail à nos familles et amis

Chapter 1

Introduction

This is, with the concluding chapter, a significant portion of memory. This should especially present the context and objectives of the work. Generally, the memory structure (content of chapters) is briefly exposed

Chapter 2

State of the art

Selective laser melting (SLM) - also referred to as direct metal laser sintering (DMLS) - is an additive manufacturing (AM) technique making use of a high power-density laser that locally melts layers of powder materials. Layers are progressively piled up, in order to create a 3D part. The technique is illustrated on figure 2.1 [10]. The materials used include mostly metals but also ceramics and composites. Parts to build must first be drawn in a computer-aided design (CAD) software and broke down in 2D slices, each one corresponding to a powder layer. During the process, the oxygen pressure p_{O_2} must be kept low to prevent the oxidation of the metal. A shielding gas - such as argon - is thus used to fill the build chamber and p_{O2} must be monitored at all time.
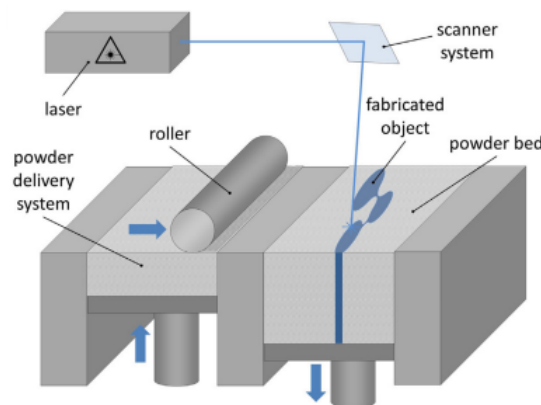
FIGURE 2.1: Selective laser melting technology principle (from Leitz et al, 2016).

LSM is still a young technology. Its popularity only increased significantly over the last decade, as depicted by figures 2.2 (a) and (b). Works concerning AlSi10Mg began to emerge noticeably in 2014. The technique usage spread rapidly in many sectors: biomedical, heat exchangers, aerospace and automotive - to name just a few [18]. This is due to the numerous appeals of LSM compared to the other technologies, including the following:

- Geometrical flexibility: parts can be designed with thin walls or even with hidden cavities and/or channels. This offers promising prospects regarding light-weight potentials for parts solicited mechanically [11];

- Increased reliability of the parts [6];

- Reduced equipment costs [7];

- Better operational efficiency: the fabrication is quick and easy which reduces time-to-market as well as assembly times and capital tied up in stocks [7];

- Individual production facilitation [6];

- Reduced material waste and better energy usage: the process is environmentally friendly as a whole [6].
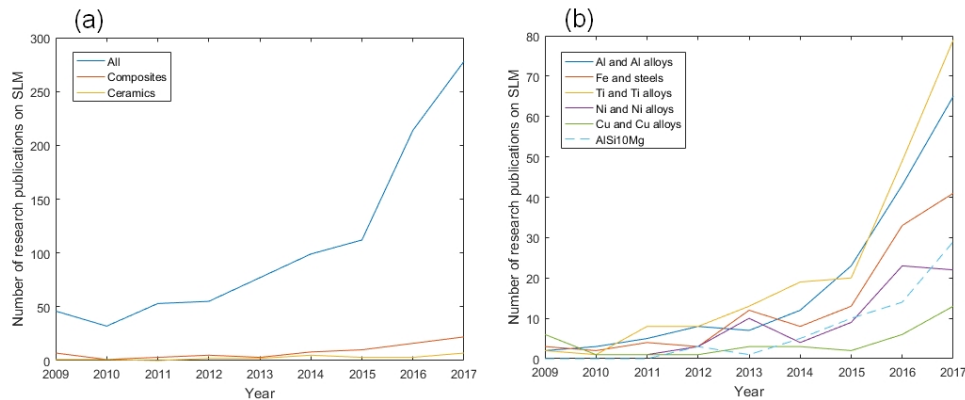

FIGURE 2.2: (a)Research publications on SLM of ceramics, composites and all materials types combined. (b)Research publications on SLM of different metallic materials. Data are derived from the research publications on SLM, LaserCusing and DMLS existing on ScienceDirect website.

Parler de l'AlSi10Mg; quel est l'interet de travailler avec? Difficultés? (reflectivité etc)

Microstructure homogène, diagramme de phase

The properties of parts produced trough SLM stem from the coupled effects of a great deal of parameters (see figure 2.3) [2]. Results are very sensitive to their variations. The process parameters must thus be monitored thoroughly. This complicates the search for their optimisation, still not fully resolved for aluminium alloys.

In recent years, works aiming at facing this challenge multiplied. The minimisation of the porosity is at the center of attention. It is indeed closely related to the quality of the mechanical properties. As porosity contributes to lowering the load-bearing surface, it reduces the apparent material strength. It was also observed to have a critical influence on the fatigue life of the produced parts. Their lifetime is especially diminished if the values of pores amount and size go beyond a certain threshold [4]. Studies investigating the effects of various parameters on the AlSi10Mg fabrication trough SLM abound in the literature.

The analysis of the paired impacts of the laser power P and scan speed v_s provides a first insight. As depicted by figures 2.4 and 2.5, low P and high v_s lead to an insufficient energy input to melt the powder and re-melt the substrate, which causes the formation of droplets [9] . The opposite leads to good penetration but also to distortions and irregularities. A trend to use both high P and v_s rose in accordance with these findings. Doing so has the advantage to increase productivity. However,
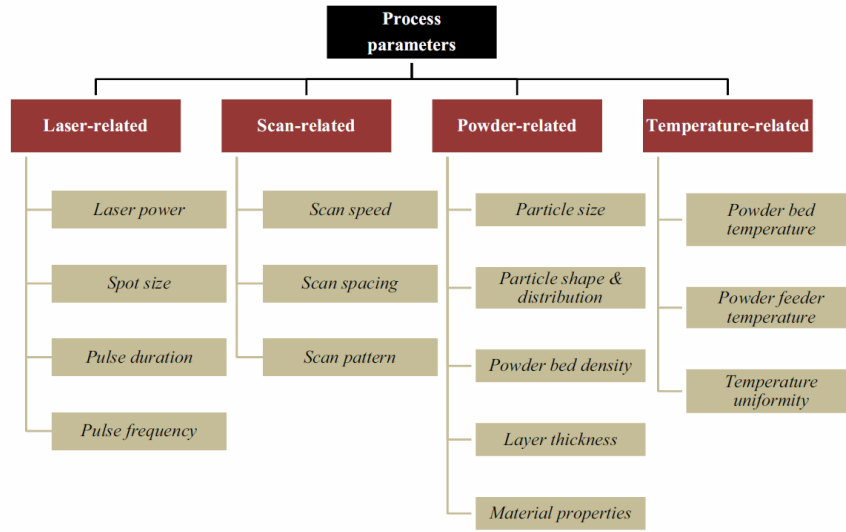
FIGURE 2.3: Parameters involved in SLM (from Aboulkhair et al, 2014).

it also has multiple downsides including a decrease of the surface quality due to balling, excessive spatter, and an augmented gas induced porosity [13]. Therefore, a trade-off must be found.

A popular approach is to regroup multiple operating parameters into one, the volumetric energy density E_d. It is estimated trough the following formula:

$$E_d = \frac{P}{v_s h t}$$

where t is the layer thickness and h is the hatch space. As a rule of thumb, E_d should be chosen in the range between 60 and 75 [$\frac{J}{mm^3}$] [15]. However, the criterion is insufficient and others should be considered such as melt pools overlapping [16]. Almost no studies were carried out to optimize h and t independently. Their values lie generally respectively in the intervals [20 ; 60] [μm] and [50 ; 200] [μm].

The other process parameters will be covered for the sake of completeness. Let us first look into the particle-related parameters. The particle size D_a of the powder should be as small as possible to ensure a good flowability and allow for thin layers [9]. Typical values stretch from 15 to 60 [μm]. The size distribution is more delicate to outline. On one hand, wider distributions often generate better bed density, parts with higher density and better surface finish. On the other hand, narrower ones usually provide better flowability and parts with better strength and hardness [12]. In most cases, a middle ground between the two should be sought. In SLM applications, powder is often successively recycled multiple times. This leads to their progressive contamination with moisture, which causes an increase of hydrogen porosity in the produced parts [17]. The problem can be overcome by drying the powder or using fresh one. Unfortunately - in the case of aluminium alloys - no findings were made regarding the prediction of a threshold at which one should take action [3].
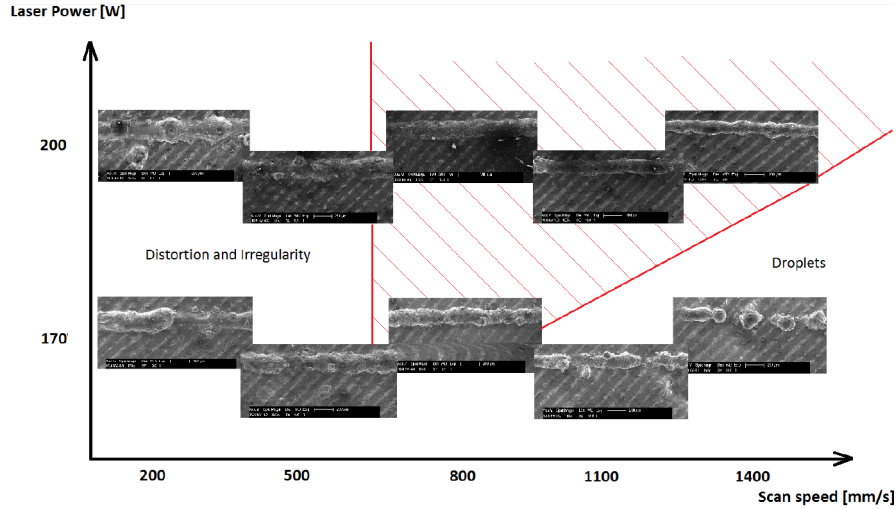
FIGURE 2.4: Process window for SLM of AlSi10Mg, based on the top view of single track scans (from Kempen et al, 2011).
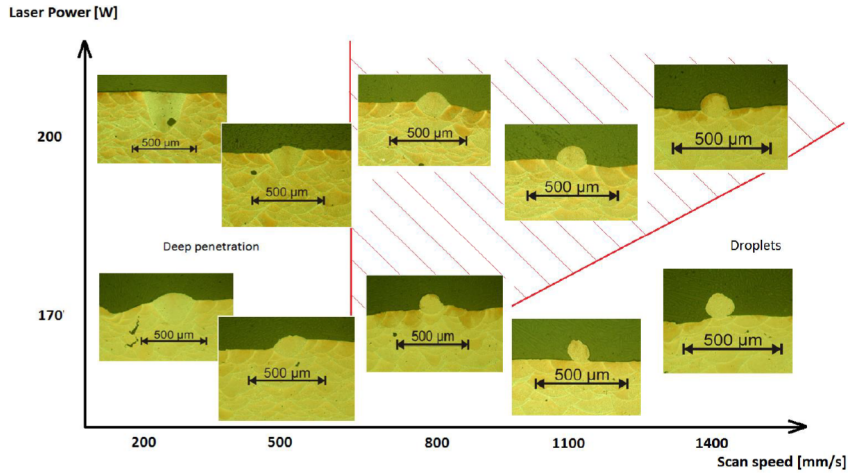
FIGURE 2.5: Process window for SLM of AlSi10Mg, based on the front view of single track scans (from Kempen et al, 2011).

The choice of scan pattern has great importance. There exist a few different strategies. The common ones use unidirectional, bidirectional or islands patterns (see figure 2.6). The scan direction(s) should be rotated between successive layers to favorise isotropy, especially in the unidirectional case since it causes height variations along a layer [1]. The islands pattern is based on a decomposition in small domains with short scanning tracks. Two usual strategies can be distinguished among this group: the chessboard and the hexagonal one.

Furthermore, dual scanning strategies were proven to be effective. For example, a pre-scan with low E_d can flatten the powder bed before it is consolidated, which leads to a reduction of porosity [13]. It was also shown that scanning the contour of the part being built at lower E_d can better the surface roughness for AlSi12Mg [14]. One should note too that the final properties of the fabricated part can strongly depend on the building direction (see figure 2.7) [5].

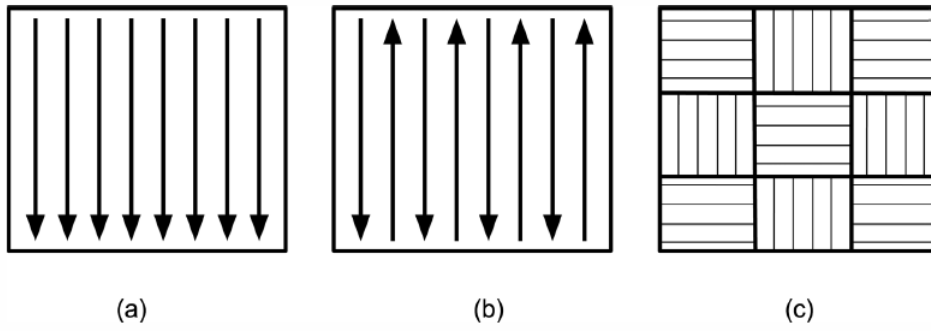FIGURE 2.6: Schematic representation of scanning strategies commonly used in LSM (a) unidirectional long scan track; (b) bidirectional long scan track, and (c) islands (from Mertens et al, 2017).
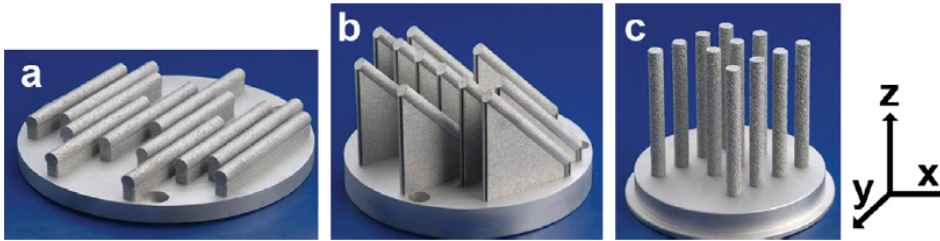

FIGURE 2.7: Samples (static tensile) built in different directions: (a) 0°, (b) 45°, and (c) 90° (from Brandl et al, 2012).

Other laser-related parameters - the spot size and the pulse properties - can also influence the process. Only the laser spot size at the 99% contour $\phi_{99\%}$ is frequently cited in literature. Its value lies between 100 and 200 $[\mu m]$.

Finally, the temperature of the powder bed and feeder affect the final properties of the fabricated parts as well. In particular, it was observed that pre-heating the powder at 300° C mitigates the differences of fatigue resistance between tensile specimens built in different directions: it is possible that the slower cooling rate induced helps reducing the distortions and internal stresses [4].

Comparer les résultats avec alliage coulé/forgé

Once the porosity problem is sorted out, other matters can be addressed such as productivity and surface roughness. The latter is problematic as the surface finish obtained with SLM is typically of such poor quality that all cracks initiate near the surface for a sample with apparent relative density $\rho_{rel} > 99\%$ [4]. As said before, it is possible to reduce the surface roughness by mean of a dual scan strategy. However, the only options to obtain significantly better surface finish is currently to machine or polish the fabricated parts. This is one of the main weak points of SLM.

Post-traitements dont traitements thermiques, sur lesquels on se focalise. Expliquer

Chapter 3

Materials and methods

Description expériences et machines

3.1 Powder follow-up

3.1.1 Sieving

3.1.2 Grain size and distribution

3.1.3 Composition

3.2 Process parameters

The same direct metal printer (DMP) was used to fabricate all specimens throughout this work. It is a *ProX DMP 200* printer, manufactured by *3D Systems* (see figure 3.1). It uses a laser with a theoritical maximal power of 300 [W] and wavelength λ = 1070 [nm] [8]. The actual maximal power is $P_{max} = 273.6$ The maximal envelope capacity of the machine (W x D x H) is 140 x 140 x 125 [mm]. Its typical accuracy is +/- 50 [μm] for small parts and +/- 0.2% for large parts. It allows for the set-up of a protection atmosphere. However, it does not integrate any heating feature for the build bed.

FIGURE 3.1: ProX DMP 200 printer (from the user's ProX DMP 200 general instructions document).

In this thesis, argon was used as shielding gas. [Corrections, paramètres laser etc...]. Values for h and t were respectively set to 100 [μm] and 30 [μm]. The other process parameters were varied so as to optimize the properties of the built specimens. Educated guesses were made based on literature and previous works done at the UCL. The parameters used are resumed in table **??**. Batches were named in the format X200-*yymmdd*. The prefix "X200" refers to the DMP used. It is followed by the date of printing (6 digits). Recycled powder was used for every batch except for X200-180222 and X200-180228. [Dual scan strategy] . Dimensions of the cubic and cylindrical specimens are noted in accordance with figure 3.2.

Batch name	Contour	Type	Dimensions [mm]	Specimen name	$\frac{P}{P_{max}}[-]$	$v_s\left[\frac{mm}{s}\right]$
X200-171024	No	Cubic	L=10	1	0.85	900
				2		1000
				3		1059
				4		1500
				5	1	900
				6		1059
				7, 7a, 7b	0.75	1200
				8, 8a, 8b		900
X200-180109	No	Cubic	L=10	7c,...7q (15 spec.)	0.75	1200
				8c,...8q (15 spec.)		900
X200-180222	No	Cubic	L=10	12	0.75	1200
				13		
X200-180228	Yes	Cylindrical	D=6, H=2	1	0.75	1200
				2		
				3		
X200180313	Yes	Cylindrical	D=6, H=10	1	0.75	1200
				2		
			D=12, H=10	3		
				4		
X200-180319	Yes	Cubic	L=10	cub 1	0.75	1200
				cub 2		
				cub 3		
				cub 4		
				cub 5		
			L=5	TT???????		
		Cylindrical	D=6, H=10	cyl 1		
				cyl 2		
			D=12, H=10	cyl 3		
				cyl 4		

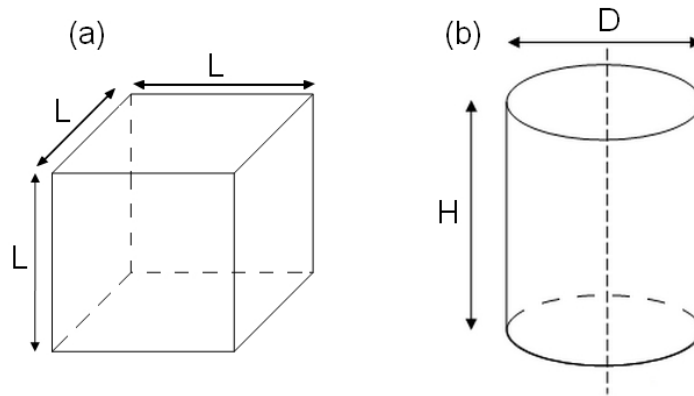TABLE 3.1: Process parameters used for the specimens manufacturing

FIGURE 3.2: Dimensions notations for (a) cubic specimens (b) cylindrical specimens

3.3 Heat treatments

3.4 Characterisation

3.4.1 Density

...

3.4.2 Microscopy

Scanning electron microscope microscopy

Optical microscopy

3.4.3 Mechanical properties

Hardness test

Traction test

Fatigue

Chapter 4

Results

Analyses statistiques etc...

4.1 Parameters optimisation

4.2 Reproducibility

4.3 Powder ageing

4.3.1 Grain size and distribution

4.3.2 Composition

Fresh powder

Recycled powder

Date of sampling	Date of last addition of fresh powder	Composition [%wt]			
		Al	Fe	Mg	Si
23/10/2017	07/09/2017	89.2	0.12	0.49	10.2
09/01/2018	07/09/2017	89.3	0.13	0.48	10.1
12/01/2018	07/09/2017	89.4	0.13	0.48	10
21/02/2018	07/09/2017 OU POUDRE NEUVE?	89.1	0.19	0.51	10.3
13/03/2018	22/02/2018	89.1	0.16	0.51	10.1

TABLE 4.1: Composition of recycled AlSi10Mg powder as a function of the date

4.4 Heat treatments

4.5 Mechanical testing

Chapter 5

Discussion

Que conclure d'après les résultats? 5.1

FIGURE 5.1: An electron (artist's impression).

Chapter 6

Conclusion

They incorporate in a synthetic way the main results and compare them with the initial objectives. Generally, this final chapter also presents prospects for the continuation of the work undertaken.

Bibliography

[1] Nesma T. Aboulkhair et al. 'On the formation of AlSi10Mg single tracks and layers in selective laser melting: Microstructure and nano-mechanical properties'. In: *Journal of Materials Processing Tech.* 230.Complete (2016), pp. 88–98.

[2] Nesma T. Aboulkhair et al. 'Reducing porosity in AlSi10Mg parts processed by selective laser melting'. In: *Additive Manufacturing* 1-4 (2014). Inaugural Issue, pp. 77 –86. URL: http://www.sciencedirect.com/science/article/pii/S2214860414000062.

[3] Nesma T. Aboulkhair et al. 'Selective laser melting of aluminum alloys'. In: *MRS Bulletin* 42.4 (2017), 311–319.

[4] Erhard Brandl et al. 'Additive manufactured AlSi10Mg samples using Selective Laser Melting (SLM): Microstructure, high cycle fatigue, and fracture behavior'. In: *Materials & Design* 34 (2012), pp. 159 –169. URL: http://www.sciencedirect.com/science/article/pii/S0261306911005590.

[5] Pauline Delroisse et al. 'Effect of strut orientation on the microstructure heterogeneities in AlSi10Mg lattices processed by selective laser melting'. In: *Scripta Materialia* 141 (2017), pp. 32 –35. ISSN: 1359-6462.

[6] Christian Haase et al. 'Exploiting Process-Related Advantages of Selective Laser Melting for the Production of High-Manganese Steel.' In: *Materials* 10(1).56 (2017).

[7] Simon Hoeges. *Additive manufacturing technologies: 6 Unique Benefits Of Selective Laser Melting*. 2017. URL: http://sintermedia.gkn.com/blog/the-advantages-of-selective-laser-melting (visited on 12/04/2018).

[8] 3D Systems Inc. *Direct metal printers: Metal Additive Manufacturing with the ProX^{TM} DMP 3D printers*. 2016. URL: http://sintermedia.gkn.com/blog/the-advantages-of-https://www.3dsystems.com/sites/default/files/2017-01/3D-Systems_DMP_Tech_Specs_USEN_2017.01.23_WEB.pdf (visited on 13/04/2018).

[9] Karolien Kempen et al. 'Microstructural analysis and process optimization for selective laser melting of AlSi10Mg'. In: *Solid Freeform Fabrication Symposium Proceedings* (2011). Conference paper, pp. 484–495. URL: https://sffsymposium.engr.utexas.edu/Manuscripts/2011/2011-37-Kempen.pdf.

[10] K.-H. Leitz et al. 'Multi-physical simulation of selective laser melting'. In: *Metal Powder Report* 72.5 (2017), pp. 331 –338. URL: http://www.sciencedirect.com/science/article/pii/S0026065716300200.

[11] Rene Lippert and Roland Lachmayer. 'A Design Method for SLM-Parts Using Internal Structures in an Extended Design Space'. In: (Sept. 2018), pp. 14–23.

[12] Bochuan Liu et al. 'Investigaztion the effect of particle size distribution on processing parameters optimisation in selective laser melting process'. In: (Jan. 2011). Conference paper, pp. 227–238.

[13]   Anne I. Mertens, Jocelyn Delahaye and Jacqueline Lecomte-Beckers. 'Fusion-Based Additive Manufacturing for Processing Aluminum Alloys: State-of-the-Art and Challenges'. In: *Advanced Engineering Materials* 19.8 (2017), p. 1700003. URL: https://onlinelibrary.wiley.com/doi/abs/10.1002/adem.201700003.

[14]   K.G. Prashanth, S. Scudino and J. Eckert. 'Defining the tensile properties of Al-12Si parts produced by selective laser melting'. In: *Acta Materialia* 126 (2017), pp. 25 –35. URL: http://www.sciencedirect.com/science/article/pii/S135964541630982X.

[15]   Noriko Read et al. 'Selective laser melting of AlSi10Mg alloy: Process optimisation and mechanical properties development'. In: *Materials & Design (1980-2015)* 65 (2015), pp. 417 –424. URL: http://www.sciencedirect.com/science/article/pii/S0261306914007468.

[16]   Ming Tang, P. Chris Pistorius and Jack L. Beuth. 'Prediction of lack-of-fusion porosity for powder bed fusion'. In: *Additive Manufacturing* 14 (2017), pp. 39 –48. URL: http://www.sciencedirect.com/science/article/pii/S2214860416300471.

[17]   Christian Weingarten et al. 'Formation and reduction of hydrogen porosity during selective laser melting of AlSi10Mg'. In: *Journal of Materials Processing Technology* 221 (2015), pp. 112 –120. URL: http://www.sciencedirect.com/science/article/pii/S0924013615000564.

[18]   Chor Yen Yap et al. 'Review of selective laser melting: Materials and applications'. In: 2 (Dec. 2015), p. 041101.